

Role of spacer in single- or two-step FRET: studies in the presence of two connected cryptands with properly chosen fluorophores†

Kalyan K. Sadhu,^a Soumit Chatterjee,^b Susan Sen^a and Parimal K. Bharadwaj^{*a}

Received 12th January 2010, Accepted 18th February 2010

First published as an Advance Article on the web 22nd March 2010

DOI: 10.1039/c000681e

Two cryptand molecules are connected *via p*-xyloyl, benzene-1,4-dicarboxylol and 9,10-dimethylene anthracene. Each cryptand is further derivatized with fluorophores such that electronic absorption of one fluorophore overlaps emission of the other. This way, three different systems **L**₁, **L**₂ and **L**₃ have been synthesized to get a better view of the effect on the distance in single- and two-step fluorescence resonance energy transfer (FRET) process. These molecules are probed for FRET in the presence of a metal ion as input. **L**₁ and **L**₂ exhibit poor performance in single step FRET while in the case of **L**₃, a large two-step FRET process is operational with Cu(II) or Hg(II) as input.

Introduction

The long range fluorescence resonance energy transfer (FRET) takes place between chromophores of overlapping emission and absorption bands as described by the Förster theory.¹ It is an important tool capable of providing information on structure and dynamics in macromolecules² as well as self-assembled structures.³ Different configurational designs as well as techniques for single- and two-step FRET with/without metal ions are covered in some recent reviews.⁴ We have been using aza-oxa cryptands⁵ to study FRET in the presence of transition/heavy metal ions. When two

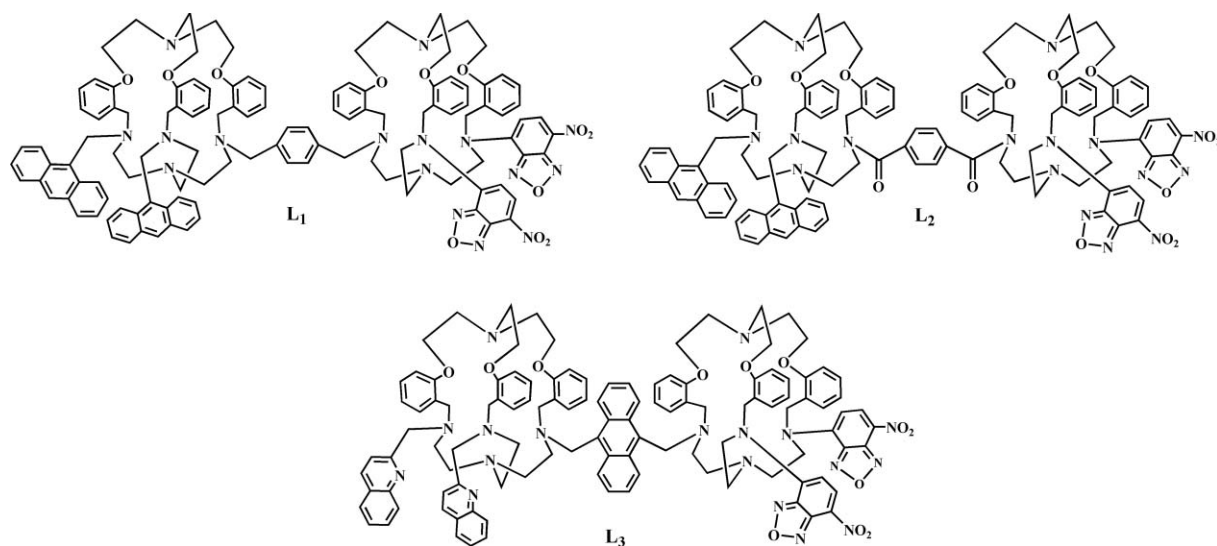
such cryptands are used to design the overall system, the nature of the spacer between the two plays a crucial role in single- and two-step FRET. To check the role of the spacer in single- and two-step FRET, we present here three different systems **L**₁–**L**₃ (Scheme 1). This study is also important from the perspective of getting valuable clues for photoinduced charge transfer processes.

In **L**₁ and **L**₂, two cryptand molecules are attached to anthracene and 7-nitrobenz-2-oxa-1,3-diazole (hereafter, diazole) with different spacers. On the other hand, in **L**₃ the two cryptands are derivatized with bis-quinoline (donor) and bis-diazoles (acceptor) and connected through 9,10-dimethylantracene spacer. The excitation and emission peaks of quinoline, anthracene and diazole are 316 and 330–400, 350 and 390–460, 475 nm and 480–540 nm respectively. This light partitioning of the fluorophores are the reason for choosing these fluorophores for the systems. This phenomenon is better explained from the schematic energy diagram (Fig. 1).

^aChemistry Department, Indian Institute of Technology Kanpur, Kanpur, 208016, India. E-mail: pkb@iitk.ac.in

^bChemistry Department, Indian Institute of Technology Bombay, Powai, Mumbai, 400076, India

† Electronic supplementary information (ESI) available: Experimental section involves characterization of the ligands **L**₁–**L**₃; Mass, ¹³C-NMR, ¹H-NMR, UV-vis and fluorescence spectral data. See DOI: 10.1039/c000681e



Scheme 1 Chemical structures of the compounds.

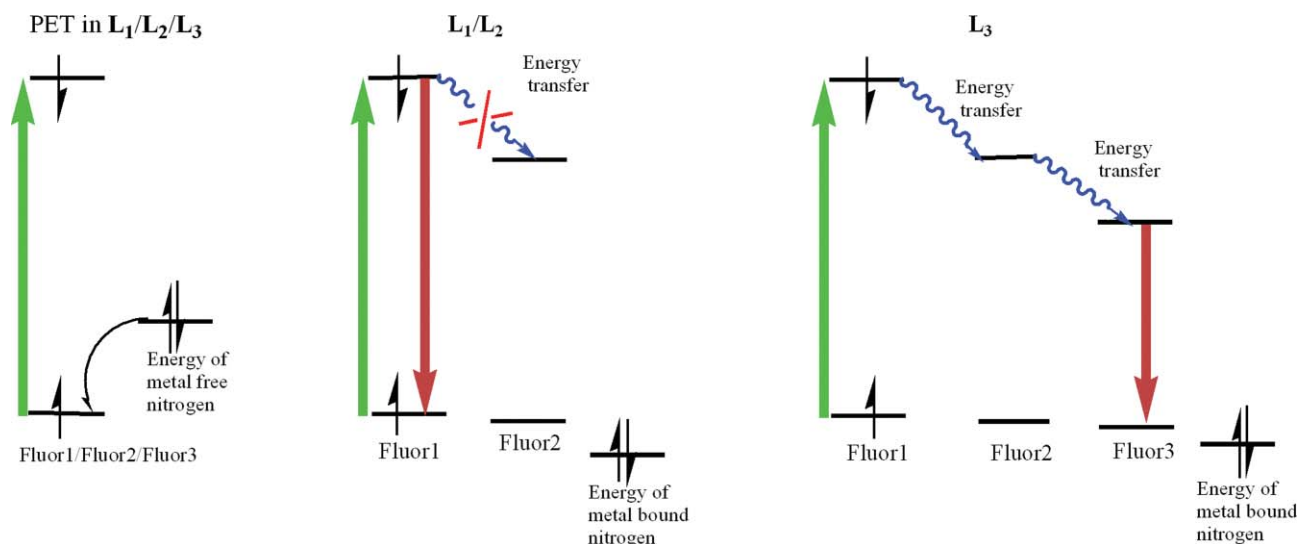


Fig. 1 An energetic diagram showing the photoinduced processes occurring in L₁, L₂ and L₃ (both in the presence and absence of metal ions).

Experimental

Materials

All solvents and thionyl chloride were purified prior to use. The purified solvents were found to be free from impurities, moisture and were transparent in the region of interest. All other reagent grade chemicals including metal salts were acquired from Aldrich that were used as received. The metal salts were hydrated as mentioned in the Aldrich catalogue. For chromatographic separation, 100–200 mesh silica gel (Acme Synthetic Chemicals) was used. The reactions were carried out under a N₂ atmosphere unless otherwise mentioned.

Synthesis

Synthesis of L₁. The synthetic route for the cryptand derivatives is illustrated in Scheme 2.

Synthesis of L₆. L₆ has been synthesized in good yield following a procedure⁶ as reported earlier from our laboratory. The crude product was recrystallized from acetonitrile as colorless crystals. This sample was used for further derivatization.

Synthesis of L₄. To a solution of L₆ (0.56 g; 1 mmol) in dry acetonitrile (20 ml), anhydrous K₂CO₃ (1.5 g, excess) was added and stirred for 15 min. Freshly recrystallized 4-chloro-7-nitrobenz-2-oxa-1,3-diazole (0.30 g, 1.5 mmol) was added to it and was allowed to reflux for 72 h. After cooling to RT, K₂CO₃ was removed by filtration. The red filtrate was evaporated to dryness under reduced pressure, washed several times with water and then extracted with CHCl₃. The organic layer, after drying over anhydrous Na₂SO₄, evaporated to dryness to obtain a red solid that was a mixture of mono-, bis- and tris-derivatives. Compound L₄ was subsequently eluted out with chloroform : methanol (98 : 2 (v/v)) as the eluent. The dark red solid obtained was recrystallized from acetone.

Yield: 45(%); mp: 130 °C; ¹H-NMR (500 MHz, CDCl₃, 25 °C, TMS, δ): 2.60–2.93 (m, 16H, 8 × CH₂), 2.98–3.11 (m, 8H, 4 × CH₂), 4.07 (s, 2H, 1 × CH₂), 4.24 (s, 4H, 2 × CH₂), 4.99 (br, 1H, NH), 6.64 (m, 4H, 4 × Ar–H), 6.75 (m, 2H, 2 × Ar–H), 6.91 (m, 1H,

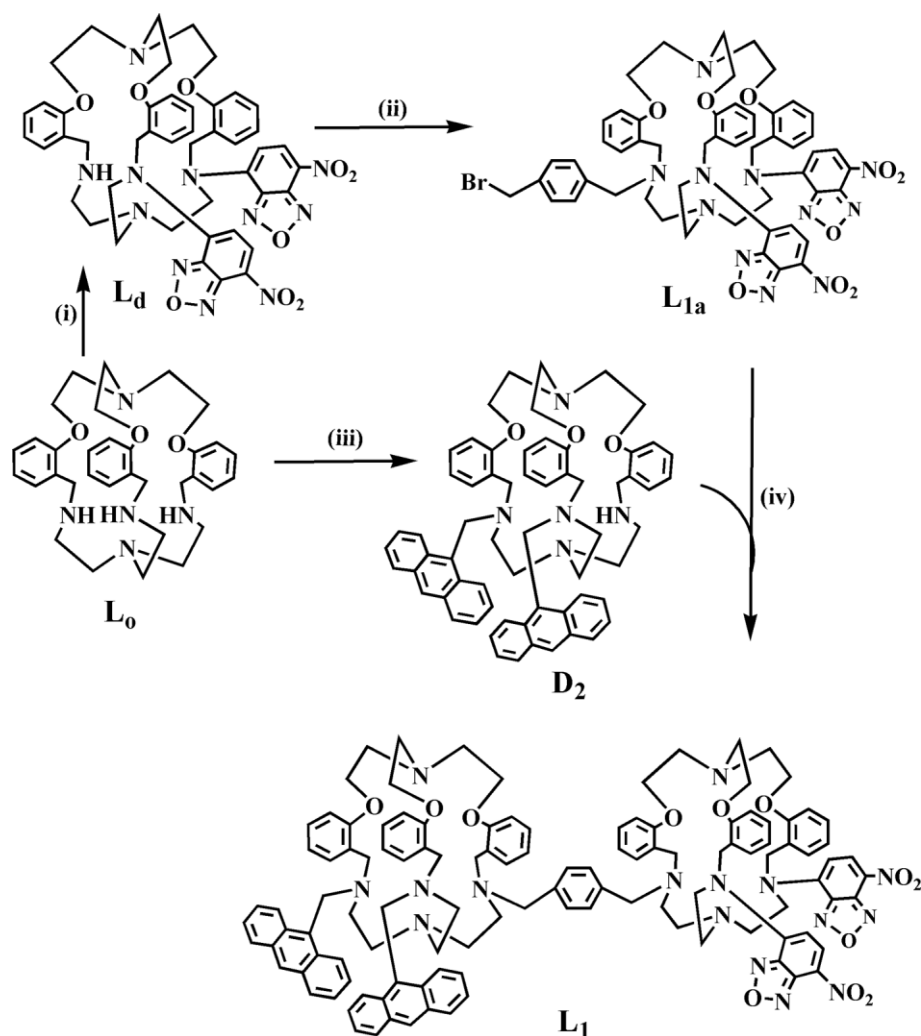
1 × Ar–H), 6.97 (d, 2H, 2 × Ar–H), 7.07 (m, 4H, 4 × Ar–H), 7.19 (m, 1H, 1 × Ar–H), 8.05 (d, 2H, 2 × Ar–H); ¹³C-NMR (125 MHz, CDCl₃, 25 °C, TMS, δ): 157.08, 155.99, 155.53, 144.70, 144.43, 144.13, 144.01, 135.12, 134.71, 131.10, 129.20, 124.46, 122.94, 122.49, 121.40, 121.09, 112.09, 111.99, 67.65, 64.71, 54.48, 48.76, 33.92, 32.02, 31.52, 30.37, 29.32, 25.99, 22.79; ESI-MS (*m/z*): 884 (75%) [L₄–1]⁺. Anal. calcd. for C₄₅H₄₇N₁₁O₉: C, 61.01; H, 5.35; N, 17.39%. Found: C, 61.10; H, 5.49; N, 17.25%.

Synthesis of L_{1a}. To a solution of L₄ (0.45 g; 0.5 mmol) in dry acetonitrile (20 ml), anhydrous K₂CO₃ (1.5 g, excess) was added and stirred for 15 min. Freshly recrystallized 1,4-bis-bromomethylbenzene (0.13 g, 0.5 mmol) was added to it along with a crystal of KI and the reaction mixture was allowed to reflux for 24 h. After cooling to RT, K₂CO₃ was removed by filtration. The red filtrate was evaporated to dryness under reduced pressure, washed several times with water and then extracted with CHCl₃. The organic layer, after drying over anhydrous Na₂SO₄, evaporated to dryness to obtain a dark red solid as L_{1a}.

Yield: 85(%); mp: 120 °C; ¹H-NMR (400 MHz, CDCl₃, 25 °C, TMS, δ): 3.03 (m, 12H, 6 × CH₂), 3.12 (m, 12H, 6 × CH₂), 4.25 (s, 6H, 3 × CH₂), 5.29 (s, 2H, CH₂), 5.96 (s, 2H, CH₂), 6.65 (m, 6H, 6 × Ar–H), 6.80 (d, 2H, Ar–H), 6.98 (m, 3H, 3 × Ar–H), 7.08 (m, 3H, 3 × Ar–H), 7.24 (m, 2H, 2 × Ar–H), 7.25 (m, 2H, 2 × Ar–H), 7.45 (d, 2H, 2 × Ar–H); ¹³C-NMR (100 MHz, CDCl₃, 25 °C, TMS, δ): 149.38, 137.66, 131.2, 129.3, 127.15, 127.76, 125.43, 124.38, 123.14, 119.60, 57.12, 49.77, 47.09, 45.08; ESI-MS (*m/z*): 1069 (35%) [L_{1a}]⁺. Anal. calcd. for C₅₃H₅₄BrN₁₁O₉: C, 59.55; H, 5.09; N, 14.41%. Found: C, 59.60; H, 5.04; N, 14.44%.

Synthesis of D₂. D₂ has been synthesized following a procedure⁷ reported earlier from our laboratory.

Synthesis of L₁. To a solution of L_{1a} (0.54 g; 0.5 mmol) in dry acetonitrile (20 ml), anhydrous K₂CO₃ (1.5 g, excess) was added and stirred for 15 min. Freshly prepared D₂ (0.47 g, 0.5 mmol) was added to it along with a crystal of KI and the reaction mixture was allowed to reflux for 24 h. After cooling to RT, K₂CO₃ was removed by filtration. The red filtrate was evaporated to dryness under reduced pressure, washed several times with water and



Scheme 2 Synthetic route to **L₁**. Reagent and conditions: (i) 4-Chloro-7-nitrobenzo-2-oxa-1,3-diazole, Toluene, reflux (ii) 1,4-bis(bromomethyl)benzene, MeCN, KI, reflux, 24 h, (iii) 9-bromomethylanthracene, MeCN, KI, reflux, 24 h and (iv) K_2CO_3 , MeCN, KI, reflux, 72 h.

then extracted with $CHCl_3$. The organic layer, after drying over anhydrous Na_2SO_4 , was evaporated to dryness to obtain a dark red solid as **L₁**.

Yield: 52%; mp: 136 °C; 1H -NMR (400 MHz, $CDCl_3$, 25 °C, TMS, δ): 1.79 (m, 48H, $24 \times CH_2$), 2.01 (m, 4H, $2 \times CH_2$), 3.32 (m, 4H, $2 \times CH_2$), 5.92 (s, 12H, $6 \times CH_2$), 6.70 (m, 4H, $4 \times Ar-H$), 7.46–7.53 (m, 16H, $16 \times Ar-H$), 8.03 (m, 6H, $6 \times Ar-H$), 8.19 (m, 6H, $6 \times Ar-H$), 8.28 (m, 6H, $6 \times Ar-H$), 8.50 (m, 6H, $6 \times Ar-H$), 9.24 (m, 6H, $6 \times Ar-H$); ^{13}C -NMR (100 MHz, $CDCl_3$, 25 °C, TMS, δ): 157.07, 155.99, 155.53, 144.69, 144.42, 144.13, 144.00, 135.12, 134.71, 131.10, 129.19, 124.45, 122.93, 122.49, 121.40, 121.08, 112.08, 111.98, 67.64, 66.19, 65.05, 64.71, 55.21, 54.48, 53.55, 48.76, 33.93, 32.02, 31.59, 30.38, 30.20, 29.60, 29.04, 28.66, 25.10, 22.79, 14.23; ESI-MS (m/z): 1928 (40% scan range 1400–2000) [**L₁**] $^+$. Anal. calcd. for $C_{116}H_{118}N_{16}O_{12}$: C, 72.25; H, 6.17; N, 11.62%. Found: C, 72.22; H, 6.18; N, 11.60%.

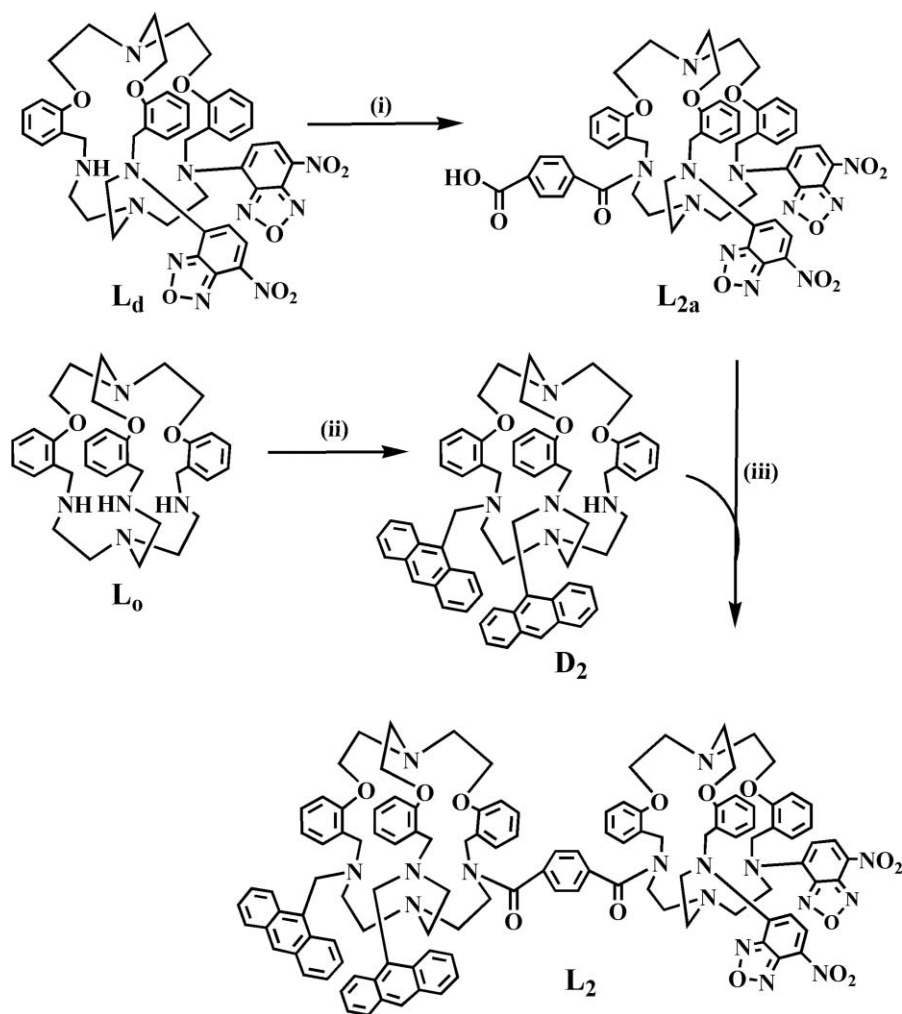
Synthesis of **L₂**. The synthetic route for this compound is illustrated in Scheme 3.

Synthesis of **L_{2a}**. To a solution of **L_d** (0.44 g; 0.5 mmol) in dry DCM (20 ml) terephthaloyl dichloride (0.11 g; 0.55 mmol)

was added and the reaction mixture was allowed to stir at room temperature for 6 h. The orange solid was filtered and washed thoroughly with DCM. Excess methanol was added for esterification of the acid chloride derivative. It was filtered and purified by column chromatography. The ester derivative was finally hydrolyzed to obtain a dark red acid derivative as **L_{2a}**.

Yield: 84%; mp: 214 °C; 1H -NMR (400 MHz, d_6 -DMSO, 25 °C, TMS, δ): 1.91 (m, 12H, $6 \times CH_2$), 2.74 (m, 4H, $2 \times CH_2$), 2.85 (m, 4H, $2 \times CH_2$), 3.25 (s, 2H, CH_2), 3.95 (m, 4H, $2 \times CH_2$), 4.15 (m, 4H, $2 \times CH_2$), 6.63 (m, 2H, $2 \times Ar-H$), 6.84 (m, 3H, $3 \times Ar-H$), 6.96 (m, 3H, $3 \times Ar-H$), 7.16 (m, 3H, $3 \times Ar-H$), 7.24 (m, 2H, $2 \times Ar-H$), 7.35 (m, 3H, $3 \times Ar-H$), 7.89 (m, 2H, $2 \times Ar-H$), 8.04 (m, 2H, $2 \times Ar-H$); ESI-MS (m/z): 1034 (40%) [**L_{2a}**] $^+$. Anal. calcd. for $C_{53}H_{51}N_{11}O_{12}$: C, 61.56; H, 4.97; N, 14.90%. Found: C, 61.62; H, 5.01; N, 14.84%.

Synthesis of **L₂**. To a solution of **L_{2a}** (0.52 g; 0.5 mmol) in dry DCM (20 ml) thionyl chloride (0.06 g, 0.5 mmol) was added and the reaction mixture was allowed to stir at room temperature for 6 h. The solvent and excess thionyl chloride were removed by evaporation under reduced pressure. The orange solid was



Scheme 3 Synthetic route to **L₂**. Reagent and conditions: (i) terephthaloyl dichloride, DCM, RT, 24 h, water (ii) 9-bromomethylantracene, MeCN, KI, reflux, 24 h and (iii) thionyl chloride, DCM, RT, 72 h.

dissolved in dry DCM and to this solution one equivalent of **D₂** was added. The final mixture was stirred for 12 h and then filtered and washed thoroughly with hot water. The product was obtained as a dark orange solid as **L₂**.

Yield: 35%; mp: 207 °C; ¹H-NMR (400 MHz, d₆-DMSO, 25 °C, TMS, δ): 1.67 (m, 48H, 24 × CH₂), 2.01 (m, 4H, 2 × CH₂), 3.11 (m, 4H, 2 × CH₂), 5.28–5.36 (m, 8H, 4 × CH₂), 6.92 (m, 3H, 3 × Ar–H), 6.97 (m, 3H, 3 × Ar–H), 7.47–7.54 (m, 24H, 24 × Ar–H), 7.99–8.05 (m, 10H, 6 × Ar–H), 8.20–8.31 (m, 6H, 6 × Ar–H), 8.52 (m, 4H, 4 × Ar–H); FAB-MS (*m/z*): 1957 (50%) [**L₂**]⁺. Anal. calcd. for C₁₁₆H₁₁₄N₁₆O₁₄: C, 71.22; H, 5.87; N, 11.46%. Found: C, 71.26; H, 5.93; N, 11.39%.

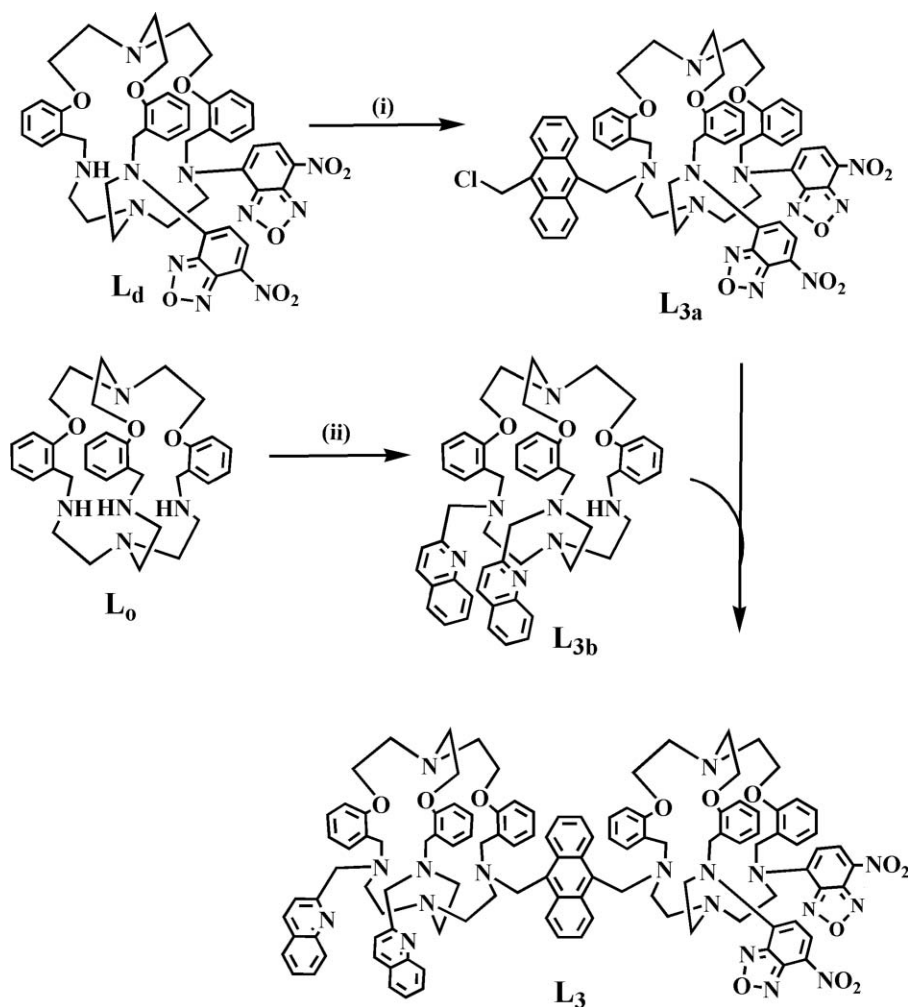
Synthesis of L₃. The synthetic route for this compound is illustrated in Scheme 4.

Synthesis of L_{3a}. To a solution of **L_d** (0.45 g; 0.5 mmol) in dry acetonitrile (20 ml), anhydrous K₂CO₃ (1.5 g, excess) was added and stirred for 15 min. Freshly recrystallized 9,10-bis-chloromethylantracene (0.14 g, 0.5 mmol) was added to it along with a crystal of KI and the reaction mixture was allowed to reflux for 24 h. After cooling to RT, K₂CO₃ was removed by filtration. The red filtrate was evaporated to dryness under reduced pressure,

washed several times with water and then extracted with CHCl₃. The organic layer, after drying over anhydrous Na₂SO₄, evaporated to dryness to obtain a dark red solid as **L_{3a}**.

Yield: 85%; mp: 118 °C; ¹H-NMR (400 MHz, CDCl₃, 25 °C, TMS, δ): 2.44 (s, 2H, CH₂), 2.45 (s, 2H, CH₂), 3.02 (m, 6H, 3 × CH₂), 3.31 (m, 12H, 6 × CH₂), 3.52 (m, 6H, 3 × CH₂), 4.63 (s, 6H, 3 × CH₂), 7.11 (m, 2H, 2 × Ar–H), 7.41–7.48 (m, 12H, 12 × Ar–H), 7.97–8.01 (m, 2H, 2 × Ar–H), 8.09–8.13 (m, 2H, 2 × Ar–H), 8.36–8.45 (m, 4H, 4 × Ar–H), 8.75–8.93 (m, 2H, 2 × Ar–H); ¹³C-NMR (100 MHz, CDCl₃, 25 °C, TMS, δ): 207.00, 157.15, 156.77, 139.24, 132.17, 130.98, 130.08, 129.88, 129.00, 128.43, 127.18, 125.35, 125.08, 120.87, 114.04, 111.19, 53.39, 33.78, 31.88, 31.60, 30.90, 29.65, 29.47, 29.33, 29.12, 28.91, 22.65, 14.09; FAB-MS (*m/z*): 1124 (50%) [**L_{3a}**]⁺. Anal. calcd. for C₆₁H₅₈ClN₁₁O₉: C, 65.15; H, 5.20; N, 13.70%. Found: C, 65.08; H, 5.22; N, 13.74%.

Synthesis of L_{3b}. To a solution of **L₀** (0.28 g; 0.5 mmol) in dry acetonitrile (20 ml), anhydrous K₂CO₃ (1.5 g, excess) was added and stirred for 15 min. Freshly recrystallized 2-bis-bromomethylquinoline (0.17 g, 0.75 mmol) was added to it along with a crystal of KI and the reaction mixture was allowed to reflux for 48 h. After cooling to RT, K₂CO₃ was removed by filtration.



Scheme 4 Synthetic route to L_3 . Reagent and conditions: (i) 9,10-bis(chloromethyl)anthracene, MeCN, KI, reflux, 48 h, (ii) 2-bromomethylquinoline, MeCN, KI, reflux, 24 h and (iii) K_2CO_3 , MeCN, KI, reflux, 72 h.

The pale yellow filtrate was evaporated to dryness under reduced pressure, washed several times with water and then extracted with $CHCl_3$. The organic layer, after drying over anhydrous Na_2SO_4 , evaporated to dryness to obtain a pale yellow solid as a mixture of mono-, bis- and tris-derivatives. The product L_{3b} was isolated by column chromatography as reported earlier.⁷

Yield: 25%; mp: 86 °C; 1H -NMR (400 MHz, $CDCl_3$, 25 °C, TMS, δ): 2.16 (m, 24H, 12 \times CH_2), 4.24 (s, 6H, 3 \times CH_2), 4.81 (m, 4H, 2 \times CH_2), 6.62 (m, 3H, 3 \times Ar-H), 6.83 (m, 4H, 4 \times Ar-H), 7.19 (m, 3H, 3 \times Ar-H), 7.35 (m, 3H, 3 \times Ar-H), 7.53 (m, 4H, 4 \times Ar-H), 7.86 (m, 3H, 3 \times Ar-H), 8.05 (m, 4H, 4 \times Ar-H); ^{13}C -NMR (100 MHz, $CDCl_3$, 25 °C, TMS, δ): 155.47, 144.42, 134.61, 123.09, 121.47, 112.09, 64.58, 32.02, 29.79, 29.45, 22.78, 14.22; ESI-MS (m/z): 842 (20%) [L_{3b}]⁺. Anal. calcd. for $C_{53}H_{59}N_7O_3$: C, 75.59; H, 7.06; N, 11.64%. Found: C, 75.50; H, 7.01; N, 11.75%.

Synthesis of L_3 . To a solution of L_{3a} (0.56 g; 0.5 mmol) in dry acetonitrile (20 ml), anhydrous K_2CO_3 (1.5 g, excess) was added and stirred for 15 min. To this mixture, L_{3b} (0.42 g, 0.5 mmol) was added along with a crystal of KI and the reaction mixture was allowed to reflux for 72 h. After cooling to RT, K_2CO_3 was removed by filtration. The red filtrate was evaporated to dryness

under reduced pressure, washed several times with water and then extracted with $CHCl_3$. The organic layer, after drying over anhydrous Na_2SO_4 , evaporated to dryness to obtain a dark red solid as L_3 .

Yield: 22%; mp: 160 °C; 1H -NMR (400 MHz, $CDCl_3$, 25 °C, TMS, δ): 1.92 (m, 48H, 24 \times CH_2), 2.25 (m, 4H, 2 \times CH_2), 3.11 (m, 4H, 2 \times CH_2), 5.09 (m, 12H, 6 \times CH_2), 7.27 (m, 6H, 6 \times Ar-H), 7.44 (m, 12H, 12 \times Ar-H), 7.48 (m, 6H, 6 \times Ar-H), 7.91 (m, 6H, 6 \times Ar-H), 8.00 (m, 6H, 6 \times Ar-H), 8.24 (m, 3H, 3 \times Ar-H), 8.45 (m, 3H, 3 \times Ar-H), 8.86 (m, 6H, 6 \times Ar-H); ^{13}C -NMR (100 MHz, $CDCl_3$, 25 °C, TMS, δ): 206.99, 139.23, 134.55, 134.08, 129.92, 127.52, 127.16, 114.02, 53.40, 33.77, 31.87, 30.89, 30.13, 29.64, 29.45, 29.31, 29.11, 28.89, 22.64, 14.09; FAB-MS (m/z): 1930 (50%) [L_3]⁺. Anal. calcd. for $C_{114}H_{116}N_{18}O_{12}$: C, 70.93; H, 6.06; N, 13.06%. Found: C, 70.82; H, 6.12; N, 13.11%.

Physical measurements

Compounds L_1 , L_2 and L_3 were characterized by elemental analyses, 1H -NMR, ^{13}C -NMR and mass (positive ion) spectroscopy. 1H -NMR and ^{13}C -NMR spectra were recorded on a JEOL JNM-LA400 FT (400 MHz and 100 MHz respectively) instrument in

CDCl₃. ESI mass spectra were recorded on a WATERS Q-TOF Premier mass spectrometer. The ESI capillary was set at 2.8 kV and the cone voltage was 30V. Melting points were determined with an electrical melting point apparatus by PERFIT, India and were uncorrected. UV-visible spectra were recorded on a JASCO V-570 spectrophotometer at 293 K and the average of three measurements was taken. The deviations in molar absorption coefficients were in the last digit only. Steady-state fluorescence spectra were obtained using a Perkin-Elmer LS 50B luminescence spectrometer at 293 K with excitation and emission band-pass of 5 nm. Steady-state fluorescence anisotropy data were obtained using a Perkin-Elmer LS 55 Fluorimeter at 293 K with a slit width of 5 nm and an integration time of 40 s. A time correlated single photon counting experiment was performed using an IBH Fluorocube spectrometer. The excitation wavelength was 295 nm. The decays were recorded at emission wavelengths of 420 nm and 526 nm at a spectral resolution of 28 ps per channel. They were fitted by the iterative de-convolution method using DAS 6.2 software. All the decays were found to be bi-exponential indicating the presence of two components, one fast and one slow, respectively.

Fluorescence quantum yields of all the compounds were determined by comparing the corrected spectrum with that of anthracene ($\phi = 0.297$) in ethanol⁸ taking the area under the total emission. On the other hand, emission quantum yields due to diazole fluorophore were checked by comparing the corrected spectrum with that of quinine sulfate⁸ in 1 N H₂SO₄. The complex stability constants K_s were determined⁹ from the change in absorbance or fluorescence intensity resulting from the titration of dilute solutions ($\sim 10^{-5}$ – 10^{-6} M) of the fluorophoric systems against metal ion concentration. The reported values gave good correlation coefficients (≥ 0.98).

Results and discussion

In dry MeCN, the absorption bands characteristic⁸ of the 9-substituted anthracene moiety of **L**₁ (Fig. 2a) in MeCN solution are observed at 349, 368 and 386 nm and the lower energy band

due to diazole is observed at 478 nm. In the case of compound **L**₂, the characteristic bands of anthracene appear at 341, 354 and 381 nm and the diazole band appears at 481 nm. The slight positional changes in the anthracene and diazole bands may be due to different spacers in **L**₁ and **L**₂. The intramolecular charge transfer (ICT) band position of diazole as well as the anthryl and quinoline band positions in **L**₃ are almost similar to our previous observation.^{5b} In **L**₃, the quinoline moiety shows a peak at 317 nm (Fig. 2b). On the other hand, the anthryl groups give a broad band centering at 377 nm with a shoulder at 392 nm without its characteristic vibrational structure. This is due to the movement and interactions between the chromophores of the side arms attached to the cryptand core.^{5a,10}

In MeCN, **L**₁ upon excitation at 350 nm, exhibits the characteristic⁹ emission band of anthracene around 420 nm and a broad emission centered at ~ 520 nm. Low intensity of emission in either case is due to photoinduced electron transfer (PET) from the tertiary nitrogen atom of the receptor to the excited fluorophore. Very similar emission behaviour is observed in **L**₂. On the other hand, **L**₃ shows triple emissions, the exact nature of which depends on the wavelength of light used for excitation. Upon excitation at 317 nm (where quinoline absorbs predominantly) in MeCN, emission due to quinoline appears at ~ 345 nm along with anthracene (~ 420 nm) and diazole (~ 520 nm) emissions. However, all the emissions are of low intensity due to PET being operational.

When a transition metal ion is added to **L**₁ in MeCN, the metal occupies¹¹ the tren-end of the cavity engaging N lone-pairs that block PET. Upon excitation at 350 nm, the quantum yield of anthracene emission increases significantly (Fig. 3a) in the presence of a transition metal or a heavy metal ion input. The extent of enhancement depends upon the nature of the metal ion (Table 1). Among the metal ions studied, Zn(II) shows the highest enhancement of anthracene fluorescence. There is also a small enhancement (within 5 times) of the diazole emission. Thus a very small amount of FRET is operating between the anthracene and diazole fluorophore, which does not change significantly in the presence of metal ion input.

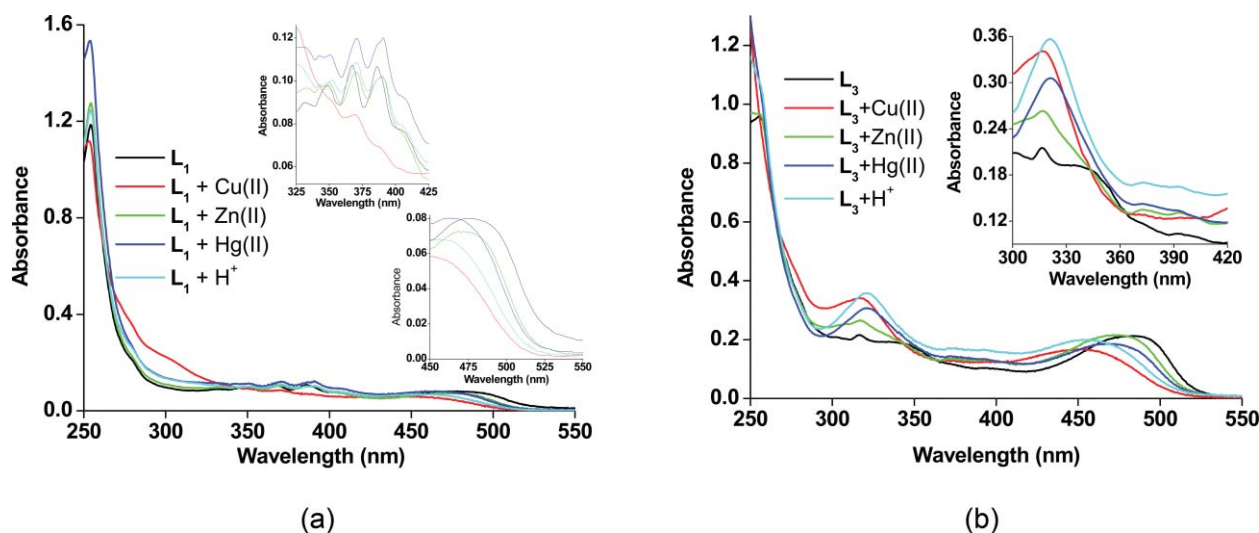


Fig. 2 (a) UV-vis spectra of **L**₁, **L**₁ + Cu(II), **L**₁ + Zn(II), **L**₁ + Hg(II), **L**₁ + H⁺ (conc. of **L**₁ = 1.7×10^{-5} M) (b) UV-vis spectra of **L**₃, **L**₃ + Cu(II), **L**₃ + Zn(II), **L**₃ + Hg(II), **L**₃ + H⁺ (conc. of **L**₃ = 1.5×10^{-5} M) in MeCN.

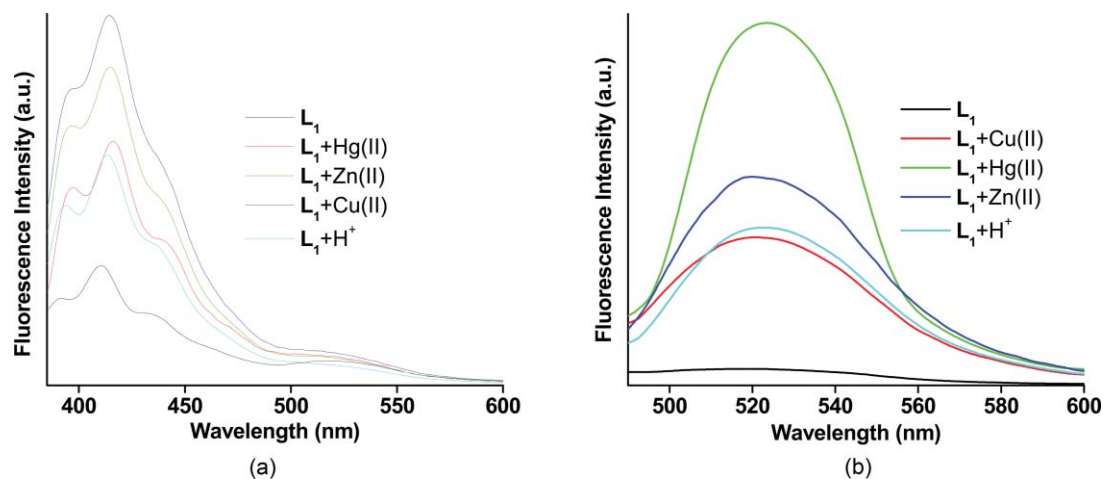


Fig. 3 Emission spectrum of L_1 , $L_1 + \text{Hg(II)}$, $L_1 + \text{Zn(II)}$, $L_1 + \text{Cu(II)}$ and $L_1 + \text{H}^+$ (conc. of $L_1 = 1.7 \times 10^{-6}$ M) excitation at (a) 350 nm and (b) 478 nm in MeCN.

Table 1 Fluorescence output of L_1 and L_2 with different ionic inputs^a **Notes:** Experimental conditions: medium, dry MeCN; concentration of ligands, $\sim 10^{-6}$ M; concentration of ionic input, 10^{-4} M; Excitation at 317 nm, 350 nm and 476 nm with excitation band-pass of 5 nm, emission band-pass, 5nm; temperature, 298 K; ϕ calculated by comparison of corrected spectrum with that of anthracene ($\phi = 0.297$) or quinine sulfate ($\phi = 0.95$) taking the area under the total emission. The error in ϕ is within 10% in each case, except free ligands, where the error in ϕ is within 15%.

Inputs	Quantum Yield ϕ (Enhancement Factor)			
	L_1		L_2	
	ϕ_{Anthr} (350 nm)	ϕ_{Diaz} (478 nm)	ϕ_{Anthr} (350 nm)	ϕ_{Diaz} (478 nm)
None	0.001	0.001	0.001	0.001
Mn(II)	0.100 (100)	0.048 (48)	0.074 (74)	0.056 (56)
Fe(II)	0.090 (90)	0.071 (71)	0.095 (95)	0.060 (60)
Co(II)	0.076 (76)	0.079 (79)	0.073 (73)	0.076 (76)
Ni(II)	0.098 (98)	0.045 (45)	0.076 (76)	0.040 (40)
Cu(II)	0.142 (142)	0.083 (83)	0.101 (101)	0.072 (72)
Zn(II)	0.148 (148)	0.094 (94)	0.088 (88)	0.112 (112)
Cd(II)	0.043 (43)	0.091 (91)	0.033 (33)	0.107 (107)
Ag(I)	0.048 (48)	0.072 (72)	0.030 (30)	0.095 (95)
Hg(II)	0.052 (52)	0.168 (168)	0.048 (48)	0.113 (113)
Pb(II)	0.094 (94)	0.101 (101)	0.066 (66)	0.102 (102)
H^+	0.044 (44)	0.064 (64)	0.025 (25)	0.040 (40)

Upon excitation of diazole fluorophore at 476 nm, there is significant fluorescence enhancement of the diazole emission in the presence of a metal ion (Fig. 3b). When a transition metal ion is added to L_2 in MeCN, quite a similar behavior as in the case of L_1 is observed although the extent of the enhancement is different (Table 1).

When L_3 is excited at 317 nm, no substantial enhancement of quinoline emission is observed. The enhancement factor remains within a limit of ~ 6 (Table 2) which is quite ineffective. Instead, two large emission bands at 420 nm and 520 nm are observed assignable to the anthracene and diazole moieties (Fig. 4) due to a significant amount of FRET from the excited quinoline to the diazole *via* anthracene where the metal ion acts as a conduit. Metal ions on coordination with the N atoms connect the different fluorophores. The highest enhancement of anthracene emission due to single-step FRET from the quinoline to the anthracene moiety is

Table 2 Fluorescence output of L_3 with different ionic inputs^a

Input	Quantum Yield ϕ (Enhancement Factor)		
	L_3 ($\lambda_{\text{ex}} = 317$ nm)		
	ϕ_{Quin}	ϕ_{Anthr}	ϕ_{Diaz}
None	0.0004	0.0014	0.0015
Mn(II)	0.0005 (1)	0.0143 (10)	0.0251 (17)
Fe(II)	0.0011 (3)	0.0369 (26)	0.0425 (28)
Co(II)	0.0011 (3)	0.0449 (32)	0.0319 (21)
Ni(II)	0.0005 (1)	0.0165 (12)	0.0218 (15)
Cu(II)	0.0015 (4)	0.1214 (87)	0.1225 (82)
Zn(II)	0.0011 (3)	0.0682 (49)	0.0451 (30)
Cd(II)	0.0014 (4)	0.0441 (32)	0.0368 (25)
Ag(I)	0.0011 (3)	0.0323 (23)	0.0198 (13)
Hg(II)	0.0022 (6)	0.2448 (175)	0.1231 (82)
Pb(II)	0.0011 (3)	0.0466 (33)	0.0363 (24)
H^+	0.0025 (6)	0.0771 (55)	0.0282 (19)

observed with Hg(II). Among the 3d-transition metal ions, Cu(II) shows a large enhancement of the anthracene monomer emission with respect to the metal free L_3 . The data are collected in Table 2. Hg(II) and Cu(II) show the highest two-step FRET in compound L_3 . Other metal ions used as input show less enhancement (Table 2). In order to verify that the fluorescence enhancement is due to the metal ion only and not because of protonation, several controlled experiments⁵ were carried out.

Since Cu(II) and Hg(II) show high quantum yields among the metal ions studied with the systems, Cu(II) is titrated with L_1 and L_2 while Hg(II) is titrated with L_3 . Both the emission bands due to the anthracene and diazole moieties are monitored for L_1 . The intensities of the anthracene emission gradually increase attaining the maximum when one equivalent of Cu(II) is added. Thereafter, no change in intensity is observed indicating a 1 : 1 formation of Cu(II) with the cryptand attached to the anthracene. During this process the quantum yield of the diazole emission increases slowly due to a small amount of FRET from anthracene to diazole. Thereafter, with an increase in concentration of Cu(II) the intensities of the diazole emission increases rapidly and it is saturated after 1 : 1 complexation of Cu(II) with the cryptand attached to the diazole. Since diazole is electron-withdrawing, the metal ion enters the cavity of the cryptand attached to the anthryl groups.¹² When L_3 is titrated with Hg(II), the emission bands due

Table 3 Interchromophoric distances of L_3 with different ionic inputs. (a) Distance between quinoline and anthracene and (b) distance between anthracene and diazole

(a)	E (%)	ϕ_a^a	$J/M^{-1}cm^3$	$\langle \kappa^2 \rangle_{max}^b$	$\langle \kappa^2 \rangle_{min}^b$	$R_{0,av}^c$	$R_{av}^{c,d}$
L_3	3	0.0030	9.02×10^{-14}	1.47	0.61	10	18
$L_3 + Cu(II)$	83	0.1586	8.89×10^{-14}	1.53	0.60	20	15
$L_3 + Hg(II)$	96	0.1397	8.27×10^{-14}	1.73	0.53	19	11
(b)	E (%)	ϕ_a^a	$J/M^{-1}cm^3$	$\langle \kappa^2 \rangle_{max}^b$	$\langle \kappa^2 \rangle_{min}^b$	$R_{0,av}^c$	$R_{av}^{c,d}$
L_3	2	0.0009	7.14×10^{-15}	1.75	0.43	11	21
$L_3 + Cu(II)$	85	0.1341	8.23×10^{-15}	2.46	0.32	14	10
$L_3 + Hg(II)$	86	0.0200	7.50×10^{-15}	1.20	0.72	18	13

^a Quantum yield of only bis-quinoline substituted cryptand in MeCN. ^{a'} Quantum yield of mono-anthracene substituted cryptand in MeCN. ^b The limits on κ^2 are obtained by the measurements of the fluorescence anisotropy of the donor and acceptor fluorophores. ^c All the distances are in Å. ^d An uncertainty in the derived intramolecular separation of approximately $\pm 15\%$ about the limit of R .

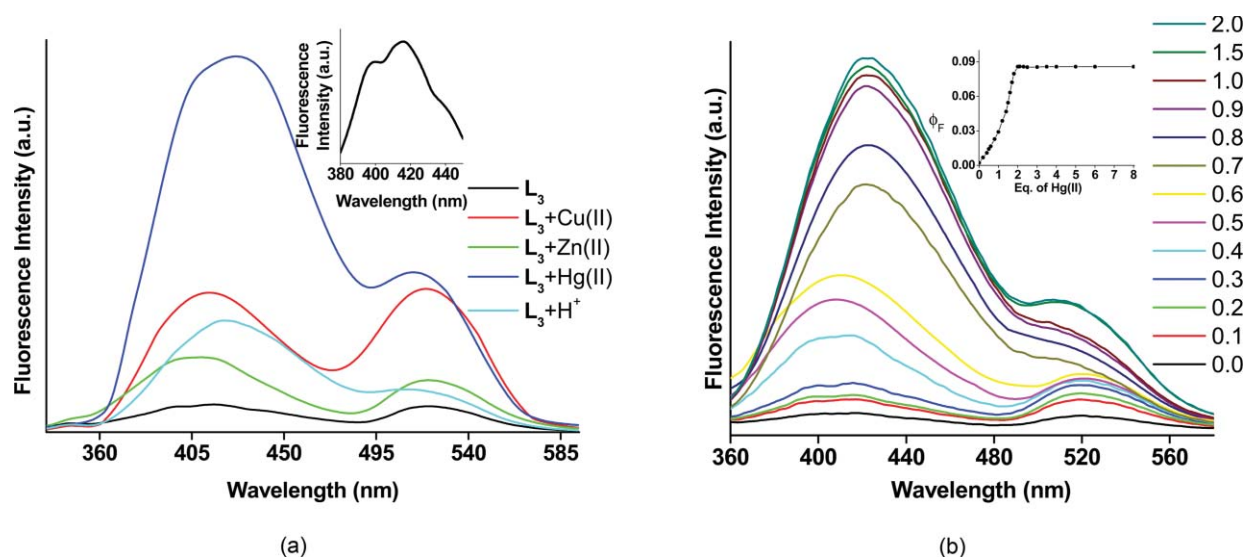


Fig. 4 (a) Emission spectrum of L_3 , $L_3 + H^+$, $L_3 + Zn(II)$ and $L_3 + Hg(II)$ (conc. of $L_3 = 1.7 \times 10^{-6}$ M) excitation at 317 nm in MeCN. (b) Emission spectra of L_3 in the presence of an increasing concentration of $Hg(II)$ in MeCN.

to anthracene and diazole moieties (Fig. 4b) are monitored and 1 : 2 formation is observed.

The binding constant (K_s) values for the cryptand moieties attached to anthracene in L_1 and L_2 with $Cu(II)$ are $1.6 \times 10^6 M^{-1}$ and $1.5 \times 10^6 M^{-1}$ respectively. The K_s values for the cryptand moieties attached to diazole in L_1 and L_2 with $Cu(II)$ are $2.4 \times 10^5 M^{-1}$ and $2.2 \times 10^5 M^{-1}$ respectively. The binding constant values suggest that at first $Cu(II)$ binds in the cryptand attached to anthracene and next to the other cryptand attached to the diazole moieties. For L_3 the overall binding constant value determined from the fluorescence intensity data with $Hg(II)$ is found to be $3.1 \times 10^{11} M^{-2}$.

The photodynamics of L_3 and its complexes were affected mostly for 420 nm emission with the incorporation of the metal ions. With the inclusion of $Cu(II)$ and $Hg(II)$, the average lifetime of the complexes were enhanced. For the $Cu(II)$ - L_3 complex, the lifetime almost doubled with an increase in the contribution of the slow component, but with a concomitant decrease in the fast component contribution. Whereas, the $Hg(II)$ - L_3 complex, at the same wavelength, the average lifetime was enhanced 1.5 times more than that of the free ligand, but with a large decrease of the slow component contribution thereby justifying the large increase in fluorescence intensity at 420 nm. At 526 nm emission, both

$Hg(II)$ and $Cu(II)$ complexes do not differ much while the average lifetime of the $Hg(II)$ complex is actually found to be slightly less than both the free L_3 ligand and the $Cu(II)$ - L_3 complex, and consequently substantiated the maximum intensity among them as found in steady-state studies. The interchromophoric distances are estimated by steady-state energy transfer experiments following a protocol reported in the literature.¹³ The distances between quinoline and anthracene, in the case of $Hg(II)$ and $Cu(II)$ complexes of L_3 , afforded values of 11 Å and 15 Å respectively. On the other hand, the distances between anthracene and diazole, in the case of $Hg(II)$ and $Cu(II)$ complexes of L_3 , afforded values of 13 Å and 10 Å respectively (Table 3).

Conclusion

In conclusion, a two-step FRET in L_3 is found to be quite significant in the presence of $Cu(II)$ and $Hg(II)$ ions. However, a single-step FRET in L_1 and L_2 is insignificant even in the presence of transition/heavy metal ions. Thus, the present systems provide a starting point to design single/multi-step FRET where a suitable choice of spacer between the donor-acceptor fluorophores is essential.

Acknowledgements

P. K. B. acknowledges the financial support from DRDO, New Delhi, India. K. K. S. and S. S. thanks the CSIR, India and S. C. thanks the UGC, India for fellowships. We thank Dr A. Datta from Indian Institute of Technology Bombay for time-resolved fluorescence and fluorescence anisotropy measurements and helpful discussions.

References

- (a) T. Förster, *Discuss. Faraday Soc.*, 1959, **27**, 7; (b) T. Förster, *Ann. Phys.*, 1948, **437**(1–2), 55.
- (a) G. Ramanoudjame, M. Du, K. A. Mankiewicz and V. Jayaraman, *Proc. Natl. Acad. Sci. U. S. A.*, 2006, **103**, 10473; (b) H. M. Watrob, C.-P. Pan and M. D. Barkley, *J. Am. Chem. Soc.*, 2003, **125**, 7336; (c) A. K. Tong, S. Jockusch, Z. M. Li, H. R. Zhu, D. L. Akins, N. J. Turro and J. Y. Ju, *J. Am. Chem. Soc.*, 2001, **123**, 12923; (d) I. L. Medintz, A. R. Clapp, H. Mattoussi, E. R. Goldman, B. Fisher and J. M. Mauro, *Nat. Mater.*, 2003, **2**, 630.
- (a) S. Kawahara, T. Uchimaru and S. Murata, *Chem. Commun.*, 1999, 563; (b) M. Cotlet, T. Vosch, S. Habuchi, T. Weil, K. Müllen, J. Hofkens and F. D. Schryver, *J. Am. Chem. Soc.*, 2005, **127**, 9760; (c) J. K. Hannestad, P. Sandin and B. Albinsson, *J. Am. Chem. Soc.*, 2008, **130**, 15889; (d) C. G. dos Remedios and P. D. Moens, *J. Struct. Biol.*, 1995, **115**, 175; K. E. Sapsford, L. Berti and I. L. Medintz, *Minerva Biol.*, 2005, **16**, 253.
- (a) E. Jares-Erijman and T. Jovin, *Nat. Biotechnol.*, 2003, **21**, 1387; (b) A. Miyawaki, A. Sawano and T. Kogure, *Nat. Cell Biol.*, 2003, S1; (c) K. E. Sapsford, L. Berti and I. L. Medintz, *Angew. Chem., Int. Ed.*, 2006, **45**, 4562; (d) R. Ziessel, M. Hissler, A. El-ghayoury and A. Harriman, *Coord. Chem. Rev.*, 1998, **178–180**, 1251; (e) B. Schlicke, L. de Cola, P. Belser and V. Balzani, *Coord. Chem. Rev.*, 2000, **208**, 267.
- (a) K. K. Sadhu, B. Bag and P. K. Bharadwaj, *Inorg. Chem.*, 2007, **46**, 8051; (b) K. K. Sadhu, S. Banerjee, A. Datta and P. K. Bharadwaj, *Chem. Commun.*, 2009, 4982.
- K. G. Ragunathan and P. K. Bharadwaj, *Tetrahedron Lett.*, 1992, **33**, 7581.
- B. Bag and P. K. Bharadwaj, *J. Lumin.*, 2004, **110**, 85.
- J. B. Birks, *Photophysics of Aromatic Molecules*, Wiley-Interscience, New York, 1970.
- (a) K. Rurack, J. L. Bricks, B. Schulz, M. Maus, G. Reck and U. Resch-Genger, *J. Phys. Chem. A*, 2000, **104**, 6171; (b) M. Kollmannsberger, K. Rurack, U. Genger-Resch and J. Daub, *J. Phys. Chem. A*, 1998, **102**, 10211.
- B. Bag and P. K. Bharadwaj, *Org. Lett.*, 2005, **7**, 1573.
- D. K. Chand and P. K. Bharadwaj, *Inorg. Chem.*, 1996, **35**, 3380.
- P. Mukhopadhyay, B. Sarkar, P. K. Bharadwaj, K. Naitinen and K. Rissanen, *Inorg. Chem.*, 2003, **42**, 4955.
- J. Mugnier, J. Pouget, J. Bourson and B. Valeur, *J. Lumin.*, 1985, **33**, 273.